Deep Learning for Structural Health Monitoring: A Damage Characterization Application

Soumalya Sarkar[1], Kishore K. Reddy[2], Michael Giering[3], and Mark R. Gurvich[4]

[1,2,3,4] *United Technologies Research Center (UTRC), East Hartford, CT, USA*
SarkarS@utrc.utc.com, ReddyKK@utrc.utc.com, GierinMJ@utrc.utc.com, GurvicMR@utrc.utc.com

ABSTRACT

Structural health monitoring (SHM) is usually focused on damage detection (e.g., Yes/No) or approximate estimation of damage size. Any additional details of the damage such as configuration, shape, networking, geometrical statistics, etc., are often either ignored or significantly simplified during SHM characterization. These details, however, can be extremely important for understanding of damage severity and estimations of follow-up damage growth risk. To avoid expensive human participation and/or over-conservative SHM decisions, solutions of computational recognition for damage characterization are needed. Autonomous SHM from visual data is one of the significant challenges in the field of structural prognostics and health monitoring (PHM). The main shortcomings of the image-based PHM algorithms arise from the lack of robustness and fidelity to handle the variability of environment and nature of damage types. In recent times, deep learning has drawn huge amount of traction in the field of machine learning and visual pattern recognition due to its superior performance compared to the state-of-the-art techniques. This paper proposes to formulate and apply a deep learning technique to characterize the damage in the form of cracks on a composite material. The deep learning architecture is constructed by multi-layer neural network that is based on the fundamentals of unsupervised representational learning theory. The robustness and the accuracy of the approach is validated on an extensive set of real image data collected via applying variable load conditions on the structure. The paper has shown a high characterization accuracy over a wide range of loading conditions with limited number of labeled training image data.

1. INTRODUCTION

Structural Health Monitoring (SHM) encompasses an umbrella of multi-disciplinary activities such as damage detection, damage quantification, damage monitoring and damage prognostics. Any additional fidelity of the damage such as configuration, shape, topological networking, geometrical statistics, etc., are often either ignored or significantly simplified during SHM characterization due to limited resources. These detailed information can however play a vital role in damage prognostics and remaining useful life (RUL) calculation of a material part. Autonomous SHM via computational recognition for damage from visual data is a necessity to avoid expensive human intervention and/or over-conservative SHM decisions.

Image processing has been an important tool in material/structural characterization for over three decades (Krakow, 1982; Duval et al., 2014; Robertson et al., 2011; Leach, 2013). Texture analysis (Comer & Delp, 2000)and segmentation (Ruggiero, Ross, & Porter, 2015; Park, Huang, Ji, & Ding, 2013) are few image processing techniques that have been used to address some of the challenges in material characterization. Pre-processing steps like filtering and enhancement techniques (Tomasi & Manduchi, 1998; Angulo & Velasco-Forero, 2013; Buades, Coll, & Morel, 2005) have been used to denoise the image and perform alignment and artifact correction.

Deep learning is one of most recent major breakthroughs in the area of image processing. The recent success of the deep learning architecture can be largely attributed to the strong emphasis on modeling multiple levels of abstractions (from low-level features to higher-order representations, i.e., features of features) from the visual data (Erhan, Courville, & Bengio, 2010; Bengio, Courville, & Vincent, 2013). Neural network and deep learning based image clustering and segmentation approaches have been extensively used in multimodal medical images (Hall et al., 1992; Özkan, Dawant, & Maciunas, 1993; Cagnoni, Coppini, Rucci, Caramella, & Valli, 1993; Liao, Gao, Oto, & Shen, 2013; Prasoon et al., 2013), which has a similarity to the structural characterization problems from an image processing perspective. To the best of the authors' knowledge, there are not many significant literatures which deal with the application of deep learning on structural characterization. In 2015, Sarkar et al. (Sarkar, Lore, Sarkar, Ramanan, et al., 2015; Sarkar, Lore, & Sarkar, 2015) adopted deep learning for vision-based PHM.

This paper proposes to formulate and apply a deep learning technique to characterize the damage in the form of cracks on a composite material. The main challenges that the authors address are: (i) extensive heuristics for parameter tuning in existing vision-based crack detection tools (Chambon, Gourraud, Moliard, & Nicolle, 2010; Oliveira & Correia, 2009), (ii) limited availability of annotation causing small training data size, and (iii) robustness issue in computer vision (segmentation) techniques. The proposed deep learning architecture, more specifically a deep autoencoder (DAE) (Bengio, Lamblin, Popovici, Larochelle, et al., 2007) is constructed by multi-layer neural network based on the fundamentals of unsupervised representational learning theory. A guided segmentation algorithm, introduced by one of the authors (Reddy et al., 2012), is applied on the transformed output of DAE to build a robust framework for damage caracterization. The performance of the approach is tested in terms of relevant metrics on an extensive set of real images collected via applying variable load on composite structure.

The paper is organized in five sections, including the present one. Section 2 describes the experimental setup and data collection method, which serves as a test apparatus for experimental validation of the proposed architecture for damage characterization. Section 3 describes the proposed framework along with its building blocks via explaining the concepts of DAE. Section 4 presents the capability and advantages of the proposed approach. Finally, the paper is summarized and concluded in Section 5 with selected recommendations for future research.

2. EXPERIMENTAL SETUP

Demonstration of the developed capabilities was performed on an example of thick multi-layer composite sub-elements used in numerous rotorcraft and aircraft applications. Such structural elements are usually under conditions of multi-axial loading with dominant influence of bending, generating complex patterns of internal damages. For demonstration purposes, simplified coupons were considered under conditions of five-point bending (Gurvich, Clavette, & Robeson, 2016). The coupons were fabricated using commercially available carbon fiber polymer-matric composite IM7/977-3 materials with lay-up $[+45_4/-45_4/0_3]_{2S}[0_3/-45_4/+45_4]$ representing quite significant thickness (0.290 in) and number of layers (55). Test implementation is illustrated in figure 1a (Gurvich et al., 2016). It indicates (1b) the complex nature of the damage network consisting of numerous, predominantly interlaminar cracks of different length, shapes, locations and mutual arrangement. The experiment was recorded as a video with moderate frame rate. The video starts with a straight coupon and slowly it is bent under monotonically increasing displacement-controlled load till full fracture happens. Image frames with different extent of cracks from the video are studied for damage characterization. Their purely manual characterization would require significant efforts and would be potentially associated with limited accuracy. Although manual differentiation of individual interlaminar cracks seems to be an obvious task, their automatic assessment may require computational implementations where deep learning solutions can be especially beneficial.

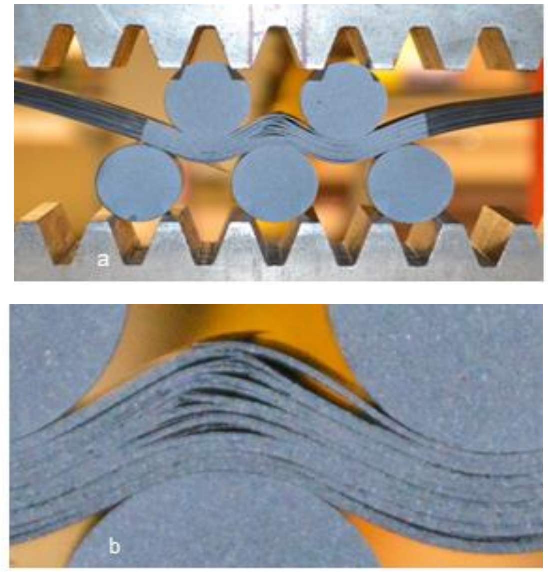

Figure 1. (a) Scheme of coupon testing and (b) representative damage pattern

3. FRAMEWORK FOR DAMAGE CHARACTERIZATION

This section describes the proposed architecture and methods, as shown in figure 2, for monitoring structural health from image data. The framework, which is built upon the concepts of machine learning, is explained in the context of a realistic problem described in the previous section with experimental data. The main objective is to automatically detect and anotate the cracks on images in real-time, which originates on the surface dynamically. The final output is the damage characterization in the form of distribution of crack lengths.

In the proposed framework, a deep autoencoder (DAE) is first trained on initial (nominal) frames of the experiment without any cracks on the surface of the coupon. The architecture and patch-wise training procedure of the DAE is described in the following subsection. Once the parameters (weights and biases) of the DAE are optimized based on the nominal surface of the material, the frame with cracks are fed into the DAE in a patch-wise fashion. The reconstruction error is obtained by subtracting the real image from the reconstructed image at the output neural layer of the DAE. The reconstruction error shows high value (visualized by whitened pixels on the

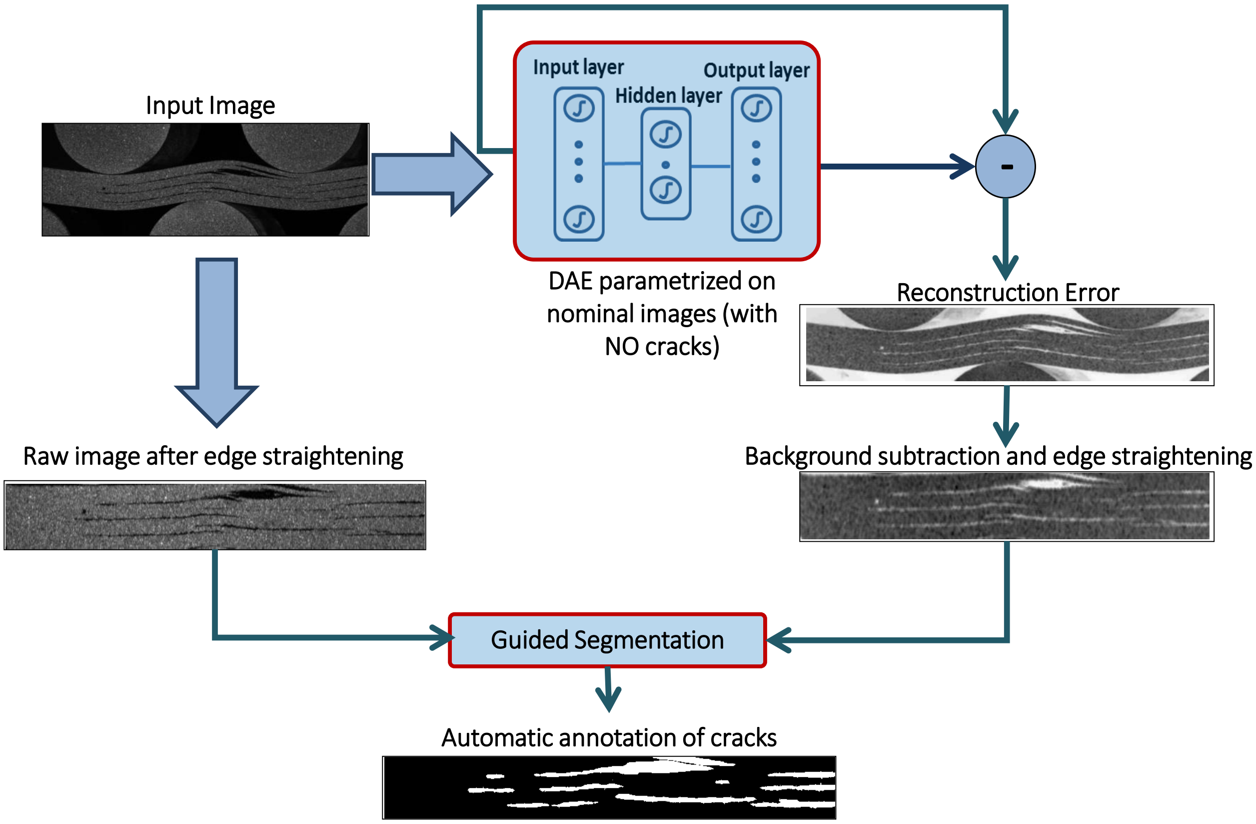

Figure 2. Framework for damage characterization

reconstruction error map at figure 2) at the background, and more importantly at the cracks. This happens because the DAE is trained only on the nominal surface image. After the background subtraction and dynamic edge straightening, reconstruction error map denotes the zones of cracks with high intensity pixels located at initial co-ordinates. Eventually, the reconstruction error map goes through a guided segmentation algorithm as a confidence map for annotating the cracks on a raw image. The region-growing guided segmentation procedure is explained later in this section. DAE offers the required robustness to crack detection via providing a confidence map to the guided segmentation tool. Without a confidence map, the annotated cracks will be fragmented leading to an erroneous crack-length distribution and small cracks will mostly be undetected at variable load conditions.

3.1. Deep Autoencoder (DAE)

DAE is one of the pillars of deep Learning, which puts a strong emphasis on modeling multiple levels of visual abstraction (from low-level features to higher-order representations, i.e., features of features) from data (Deng & Dong, 2014; Bengio et al., 2013). For example, in a typical image processing application while low-level features can be partial edges and corners, high-level features may be combination of edges and corners to form parts of an image. In typical image reconstruction applications, an image frame is usually represented as a matrix containing color information or intensity values of all pixels. The matrix can be reshaped into a row vector as a form of low-level (e.g., pixel level) representation. The vectors are transformed as they go deeper into the model, consequently resulting in a different vector that may represent higher-level features (e.g., edges) instead. In this paper, a whole image frame is greyscale and dimension is of the order of 855×603 pixels. That's why, instead of the whole image, a patch of size 3×7 pixels is traversed over the full frame (figure 3) with $\sim 80\%$ overlap to generate a series ($\sim 10,000$) of training image vectors of dimension 21 (3×7). This skewed patch dimension (3×7 pixels) is chosen to facilitate longitudinal smoothing as the cracks propagate horizontally in the experiments. The order of patch dimension is decided based on the average transverse width of the cracks, which is $\sim 2 - 5$ pixels. These image vectors at nominal (no crack) conditions, collected from the coupon surface sections of the frames, act as a training data to DAE.

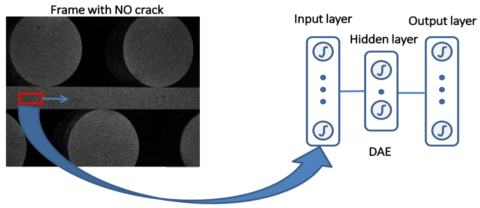

Figure 3. Application of deep autoencoder (DAE) via patching frame-by-frame

A DAE is constructed by a multi-layer neural network, where there is an input layer, single or multiple hidden layers and an output layer. Each layer can have different number of neural units as shown in the figure 3. A DAE (Bengio et al., 2007) takes an input vector $\mathbf{x} \in \mathcal{R}^d$ and first maps it to the latent representation $\mathbf{h} \in \mathcal{R}^{d'}$ using a deterministic sigmoid function of the type $\mathbf{h} = f_\theta = \sigma(Wx + b)$ with parameters $\theta = \{W, b\}$, where W is the weight and b is the bias. This "code" is then used to reconstruct the input by a reverse mapping of $f : y = f\theta'(h) = \sigma(W'h + b')$ with $\theta' = \{(W'), b'\}$. The two parameter sets are constrained to be of the form $W' = W^T$, using the same weights for encoding the input and decoding the latent representation. Each training pattern x_i is then mapped onto its code h_i and its reconstruction y_i. The parameters are optimized via stochastic gradient descent method (Bengio et al., 2007), minimizing an appropriate cost function over the training set $\mathcal{D}_n = \{(x_0, t_0), ..., (x_n, t_n)\}$. In this paper, the cost function $L(xy)$ is assumed to be the root mean square error between the input vector and reconstructed vector.

$$L(xy) = ||x - y||^2 \tag{1}$$

A DAE with three layers containing an input layer, one bottleneck layer and an output layer is considered here. The bottleneck layer consists of 10 neural nodes whereas the input and output layers contain 21 neural nodes each. The contraction in dimension at the bottleneck layer helps in reducing the over-fitting (Bengio et al., 2007) on the training data.

3.2. Region-growing Guided segmentation

The reconstruction error map of the test image acts as a robust confidence map to the guided segmentation process. Region growing (Reddy et al., 2012) is a pixel-based image segmentation method, which checks the neighbor pixels of the initially provided seed region and iteratively adds the neighbor pixels to the region to be grown if a measure of similarity $S(x, y)$ is smaller than a threshold. After adding a pixel, the mean intensity of the grown region is updated. In this algorithm, the similarity $S(x, y)$ is weighted by the confidence of that pixel being a crack, according to the confidence map. This helps the region to grow to the pixels with similar intensities and also with high confidence of being a crack. More specifically, the similarity measure is defined as $S(x, y) = |I(x, y) - c|(1 - p(x, y))$, where $p(x, y)$ is the probability (intensity of the confidence map) of a pixel being a crack, $I(x, y)$ is the raw image intensity of pixel (x, y), and c is the mean intensity of the current region. The pixels in the neighborhood of a current boundary pixel with the minimal $S(x; y)$ is included into the region. Background subtraction is also performed using this algorithm based on the reconstruction error map.

4. RESULTS AND DISCUSSIONS

This section describes the damage characterization performance results that are obtained when the proposed framework is applied on experimental images. In general image processing tasks, an important metric for good detector is formulated by how many pixels are correctly detected. But for crack detection from a damage characterization perspective, the important metrics are the number of correct cracks detected and the normalized distance between original and estimated distribution of crack lengths (say d)

After training the DAE on a nominal frame in the method explained in section 3, it is tested on frames containing cracks at variable loading level. As the load increases, the number and length of cracks also increase non-linearly. Another challenge is associated with the fact that the whole coupon also bends according to a non-linear topological deformation criteria with the increment of load. That's why, a dynamic edge straightening is required. To reduce the complexity of the whole framework, a threshold is assigned on the reconstruction error map or confidence map intensity level. If a pixel intensity is more than the threshold, it is 1 and if the intensity is lesser than the threshold, that pixel value is converted to 0. The best threshold is found to be ~ 0.55 for the medium load level crack detection,i.e., at 0.55 the framework detects most number of correct cracks with least d. First to third image from top of the figure 4 show the gradual progression of the framework functionality. The last two images are the frames with detected cracks (marked by white pixels) and the annotated ground truth respectively. Despite the cracks being only few pixels wide in the raw textured image, the validation shows that the detected crack areas cover majority ($\sim 90\%$) of the original annotated cracks.

Varying crack width ($\sim 1 - 7 pixels$) and noisy textured surface image pose another significant challenge in image processing task with respect to maintaining the longitudinal continuity of a single crack. If the longitudinal continuity is not preserved in the testing frame, the estimated number of crack will be largely different from the actual number of cracks due to lengthwise fragmentation. The proposed framework performs well in detecting the number of cracks. Figure 5

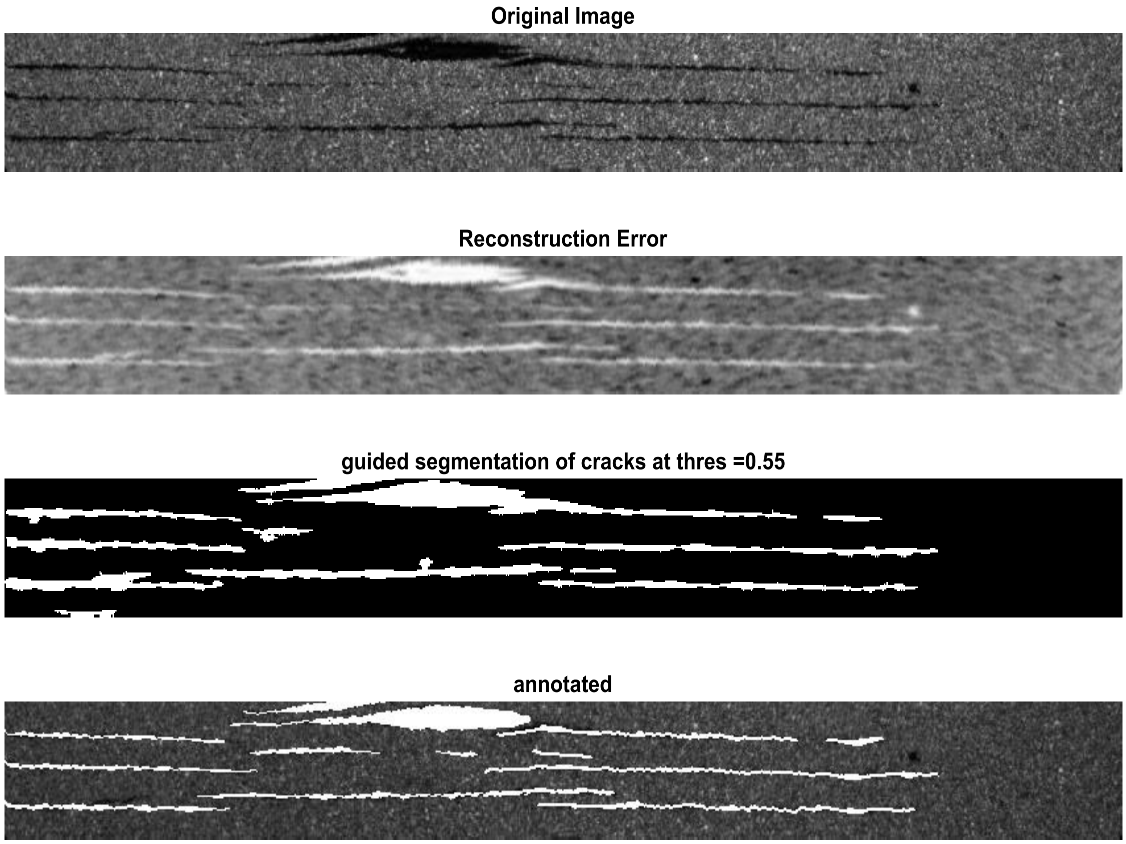

Figure 4. Validation on a frame for medium load condition. The last two images are the ones with detected crack (white pixels) and the annotated ground truth respectively

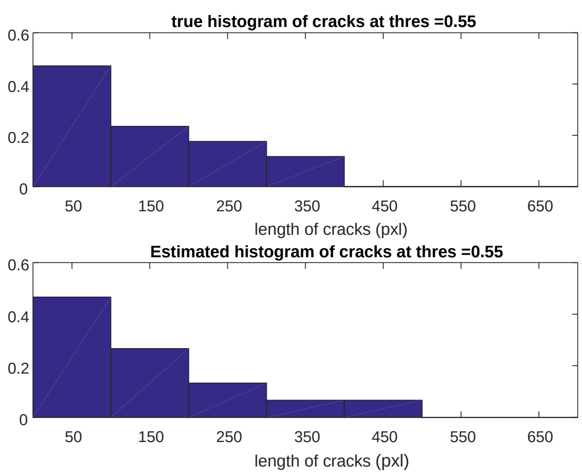

Figure 5. Comparison of estimated histogram over crack lengths and the ground truth histogram

demonstrates the estimated histogram over crack lengths and the ground truth histogram. They are satisfactorily similar with $d = 0.1$ while capturing the probabilities of larger cracks with more precision compared to that of the small ones.

The table 1 describes a range of damage characterization per-

Table 1. Comparison of damage characterization performances at variable load condition

Loading level	Number of correct cracks detected	d
low	4 out of 4	0.18
medium	16 out of 17	0.1
high	19 out of 20	0.15

formances for varying load condition in terms of the two major metrics mentioned earlier. It is observed that the framework exhibits consistancy in characterizing cracks at different level of loads. The DAE and the confidence map threshold of 0.55 are robust to changing load levels.

5. CONCLUSION AND FUTURE WORK

In this paper, the authors formulate and implement a novel framework containing deep learning to characterize the damage in the form of cracks on a composite material. The proposed framework addresses the shortcomings of existing image processing tools in relation to damage characterization, which are about lack of robustness and sensitivity to parameter heuristics. The deep autoencoder (DAE) is constructed by multi-layer neural network and optimized by stochastic backpropagation. The reconstruction error map acts as a confidence map for the guided segmentation tool to obtain the number of cracks and crack-length distribution. The characterization performance of the framework is validated in terms of relevant metrics (number of correct cracks detected and the normalized distance between original and estimated distribution of crack lengths) on an extensive set of real image frames. The image frames are parts of multiple videos collected during experiments that apply variable load on composite structures. The paper has shown a high characterization accuracy and satisfactory robustness over a wide range of loading conditions with limited number labeled training image data. Some of the near-term future tasks are:

- formulate and implement an end-to-end (from image frame to damage characterization) deep learning architecture by eliminating the separate guided segmentation module.
- Parametric tracking of non-linear topological deformation instead of heuristic edge straightening.
- Applying 3-dimensional convolutional DAE for 3-dimensional damage characterization.

A more strategic vision for the long-term future steps is to apply developed capabilities for objectives of advanced maintenance or service-related decision making, where progressive damage process is expected to be a function of time or load or both. This vision is planned to be implemented into two mutually inter-connected directions. The first one is focused on more accurate and cost-efficient characterization of damage or deformation states. Indeed, quantification of sizes, shapes, location and networking of observed damage can be performed with much higher quality by deep-learning capabilities than, for example, by manual or semi-manual measurements. Another direction of improved damage monitoring is envisioned to take into account a significantly larger population of individual parameters, including numerous details of the damage state as illustrated, for example, in the present paper. Larger population of such parameters can provide high probability of down-selection of the most informative metrics with higher sensitivity to the damage process. Therefore, robustness of damage monitoring can be signigificantly enhanced with follow-up opportunities to reduce conservatism of service and/or maintenance requirements. More systematic results in this area will be presented in a coming separate publication.

ACKNOWLEDGMENT

The authors thank United Technologies Research Center (UTRC) for funding of this study and permission for publication and Mr. Patrick Clavette for experimental implementation of the demonstration case.

REFERENCES

Angulo, J., & Velasco-Forero, S. (2013). Stochastic morphological filtering and bellman-maslov chains. In *Mathematical morphology and its applications to signal and image processing* (pp. 171–182). Springer.

Bengio, Y., Courville, A., & Vincent, P. (2013). Representation learning: A review and new perspectives. *Pattern Analysis and Machine Intelligence, IEEE Transactions on*, *35*(8), 1798–1828.

Bengio, Y., Lamblin, P., Popovici, D., Larochelle, H., et al. (2007). Greedy layer-wise training of deep networks. *Advances in neural information processing systems*, *19*, 153.

Buades, A., Coll, B., & Morel, J.-M. (2005). A non-local algorithm for image denoising. In *Computer vision and pattern recognition, 2005. cvpr 2005. ieee computer society conference on* (Vol. 2, pp. 60–65).

Cagnoni, S., Coppini, G., Rucci, M., Caramella, D., & Valli, G. (1993). Neural network segmentation of magnetic resonance spin echo images of the brain. *Journal of biomedical engineering*, *15*(5), 355–362.

Chambon, S., Gourraud, C., Moliard, J. M., & Nicolle, P. (2010). Road crack extraction with adapted filtering and markov model-based segmentation: introduction and validation. In *International joint conference on computer vision theory and applications, visapp.*

Comer, M. L., & Delp, E. J. (2000, Oct). The em/mpm algorithm for segmentation of textured images: analysis and further experimental results. *IEEE Transactions on Image Processing*, *9*(10), 1731-1744. doi: 10.1109/83.869185

Deng, L., & Dong, Y. (2014). Foundations and trends® in signal processing. *Signal Processing*, *7*, 3–4.

Duval, L., Moreaud, M., Couprie, C., Jeulin, D., Talbot, H., & Angulo, J. (2014, Oct). Image processing for materials characterization: Issues, challenges and opportunities. In *2014 ieee international conference on image processing (icip)* (p. 4862-4866). doi: 10.1109/ICIP.2014.7025985

Erhan, D., Courville, A., & Bengio, Y. (2010). Understanding representations learned in deep architectures. *Département d'Informatique et Recherche Operationnelle, University of Montreal, QC, Canada, Tech. Rep*, *1355*.

Gurvich, M. R., Clavette, P. L., & Robeson, M. E. (2016). Approach of Interlaminar Characterization for Thick Aircraft Composite Structures. In *57th aiaa/asce/ahs/asc structures, structural dynamics, and materials conference, aiaa scitech, paper aiaa 2016* (pp. 1235–1243).

Hall, L. O., Bensaid, A. M., Clarke, L. P., Velthuizen, R. P., Silbiger, M. S., & Bezdek, J. C. (1992). A comparison of neural network and fuzzy clustering techniques in segmenting magnetic resonance images of the brain.

Neural Networks, IEEE Transactions on, *3*(5), 672–682.

Krakow, W. (1982). Image-processing for materials characterization. In *Journal of metals* (Vol. 35, pp. A42–A42).

Leach, R. K. (2013). *Characterisation of areal surface texture*. Springer.

Liao, S., Gao, Y., Oto, A., & Shen, D. (2013). Representation learning: A unified deep learning framework for automatic prostate mr segmentation. In *Medical image computing and computer-assisted intervention–miccai 2013* (pp. 254–261). Springer.

Oliveira, H., & Correia, P. L. (2009, Aug). Automatic road crack segmentation using entropy and image dynamic thresholding. In *Signal processing conference, 2009 17th european* (p. 622-626).

Özkan, M., Dawant, B. M., & Maciunas, R. J. (1993). Neural-network-based segmentation of multi-modal medical images: a comparative and prospective study. *Medical Imaging, IEEE Transactions on*, *12*(3), 534–544.

Park, C., Huang, J. Z., Ji, J. X., & Ding, Y. (2013, March). Segmentation, inference and classification of partially overlapping nanoparticles. *IEEE Transactions on Pattern Analysis and Machine Intelligence*, *35*(3), 1-1. doi: 10.1109/TPAMI.2012.163

Prasoon, A., Petersen, K., Igel, C., Lauze, F., Dam, E., & Nielsen, M. (2013). Deep feature learning for knee cartilage segmentation using a triplanar convolutional neural network. In *Medical image computing and computer-assisted intervention–miccai 2013* (pp. 246–253). Springer.

Reddy, K. K., Solmaz, B., Yan, P., Avgeropoulos, N. G., Rippe, D. J., & Shah, M. (2012, May). Confidence guided enhancing brain tumor segmentation in multi-parametric mri. In *2012 9th ieee international symposium on biomedical imaging (isbi)* (p. 366-369). doi: 10.1109/ISBI.2012.6235560

Robertson, I. M., Schuh, C. A., Vetrano, J. S., Browning, N. D., Field, D. P., Jensen, D. J., ... others (2011). Towards an integrated materials characterization toolbox. *Journal of Materials Research*, *26*(11), 1341–1383.

Ruggiero, C., Ross, A., & Porter, R. (2015). Segmentation and learning in the quantitative analysis of microscopy images. In *Is&t/spie electronic imaging* (pp. 94050L–94050L).

Sarkar, S., Lore, K. G., & Sarkar, S. (2015). Early detection of combustion instability by neural-symbolic analysis on hi-speed video. In *Proceedings of the nips workshop on cognitive computation: Integrating neural and symbolic approaches; 29th annual conference on neural information processing systems (nips 2015).*

Sarkar, S., Lore, K. G., Sarkar, S., Ramanan, V., Chakravarthy, S. R., Phoha, S., & Ray, A. (2015). Early detection of combustion instability from hi-speed flame images via deep learning and symbolic time series analysis. In *Annual conference of the prognostics and health management society 2015.*

Tomasi, C., & Manduchi, R. (1998). Bilateral filtering for gray and color images. In *Computer vision, 1998. sixth international conference on* (pp. 839–846).